Flood Risk and Climate Change Hokkaido

WP2 Bank failure probability

Client

Partners for Water

Flood Risk and Climate Change Hokkaido

WP2 Bank failure probability

Final report

Authors
Fumihiko, UEMURA (Docon Co.,Ltd)
Rongen, Guus (HKV consultants)

PR3983
January 2022

Table of contents

1 Introduction

This report gives an overview of the activities from work package 2 (WP2). This work package is one of the three work packages that gives insight in the flood risk for Hokkaido and specifically the case study Obihiro. WP1 gives insight in the impact of climate change on extreme water levels, WP2 focusses on probability of levee failure.

The probability of flood occurrence consists of the effects of the probability of water level exceedance and the probability of dike failure. The method of calculating and analyzing the probability of water level exceedance is described in the WP1 report. In this report, only the results of the calculation of the probability of water level exceedance are described.

For the probability of dike failure, a fragility curve is calculated by focusing on the mechanism of levee failure due to water overflow. Uncertainty is included in the fragility curve. Uncertainty takes into account the relationship between water level and flow rate, the height of the planned and actual levees, and the condition of the grass on the surface of the levees.

1.1 Objective

The objective of work package 2 is to determine the flood probability for the Obihiro case and give insight in the uncertainties in bank failure probability calculation.

1.2 Structure report

The report starts with an overview of the targeted failure mechanisms and the approach taken to analyze them probabilistically (Chapter 2). Chapter 3 describes the target basins and districts, and explains the concept of longitudinal classification of assessments. Chapter 4 describes the physical conditions that cause failure and how to create a fragility curve. Chapter 5 describes the uncertainties included in the fragility curve. These are: water level (5.1), bank height (5.2), and inner slope condition (5.3). The failure probability is calculated in Chapter 6. Here, a method is also proposed to take into account the upstream probability (6.2) In Chapter 7, the flood probability is calculated, including the flow statistics provided by WP1. In Chapter 8, sensitivity analysis was conducted on the uncertainty included in the fragility curve and the shape of the hydrograph. Finally, the characteristics of the results obtained from this method and future prospects are discussed (Chapter 9), and conclusions are provided in Chapter 10.

2 Method

In flood control planning in Japan, calculations are based on the condition that a breach will occur if the water level exceeds the planned water level. The probability is evaluated as 0 or 1, whether the water level will be exceeded or not. However, the actual phenomenon of breaching is that the water level may reach the planned water level but not breach, or the water level may not reach the planned water level but breach occurs. This is due to various factors such as the mechanism of levee failure, strength of the levee, and temporal changes in hydraulic conditions. Probabilistic assessment of levee failure is essential for the correct assessment of flood risk.
In the Netherlands, flood risk has been assessed based on the probability of levee failure using a fragility curve, which has been introduced into policy.
In this study, the Dutch method of calculating the probability of breaching is applied to the Tokachi River basin, and a method of creating a fragility curve is proposed, with some modifications based on the characteristics of floods in Japan.

2.1 Mechanism of dike failure

There are several factors that can cause levee breaches. In Japan, the factors are generally divided into overflow, erosion/ scour, and seepage. In 2019, typhoon No. 19 caused floods in Japan and breaches of levees occurred in many places, including 14 on rivers managed by the national government and 128 on rivers managed by prefectural governments. According to the results of a survey on the causes of breaches, overflowing water was the main cause of 86% of the breaches [6]. In this study, the probability of levee breakage was calculated for overflowing water, which is one of the most frequently reported causes of levee breakage in Japan.

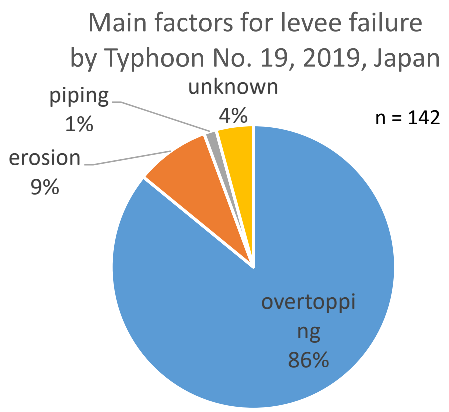

- In the case of the floods caused by Typhoon No. 19 in Japan, levee failures occurred in 14 national rivers and 128 prefectural rivers.
- The main factor for the failure is overtopping of water, which accounts for 86%.

Based on Reference [6].

Figure 1 Causes of the levee failure caused by Typhoon No. 19 2019, in Japan .

2.2 Overview of the our approach

The method applied in this study is based on VNK2 [8] and the Dutch method for dike safety assessment, called BOI [9]. Adjustments have been made to some parts of the method:

- Only the failure mechanism overtopping was considered, as it is considered the most important for Obihiro. We applied a cumulative damage approach, to take into account the duration of overtopping.
- Not only the probabilities of the peak discharges are considered, but also the shape of the hydrograph. A high water level with a long duration gives a higher failure probability, as it can cause more damage to the revetment.
- When calculating the total failure probability for the area, we use a tailored approach to take dependencies between different dike sections into account.

    1. Failure probabilities are combined conditional to the discharge, as different sections would fail during the same high discharge conditions.
    2. For combining segments into section probabilities, the maximum segment failure probability per discharge is used, hence, the segments are considered dependent.
    3. When combining sections to river probabilities, the reducing effect of potential failure of upstream sections is taken into account.

The definition of segments and sections is explained in chapter 3.

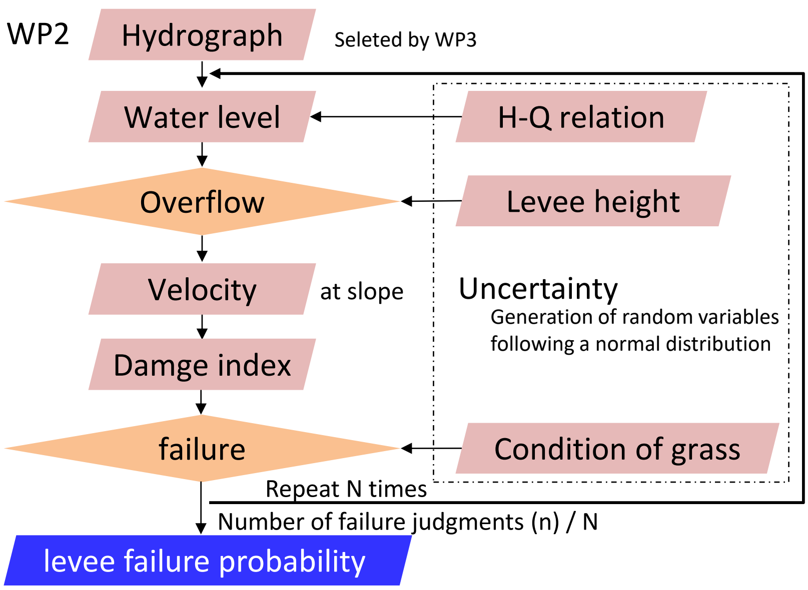

Figure 2
Flow of calculation of breach probability considering uncertainty.

3 Target basin

In this study, the levees of the Tokachi River and the Satsunai River adjacent to the Obihiro urban area are evaluated. An overview of this area is shown below.

Data are collected at intervals of about 0.2 km in the target rivers, indicated with the circles in the figure. In this study, the levee segments are evaluated at the same interval. The sections (i.e., a collection of segments) are shown with different colors. The segment within the section that is considered in WP3, is shown with a black cross. The KP number for these breach locations are shown as well.

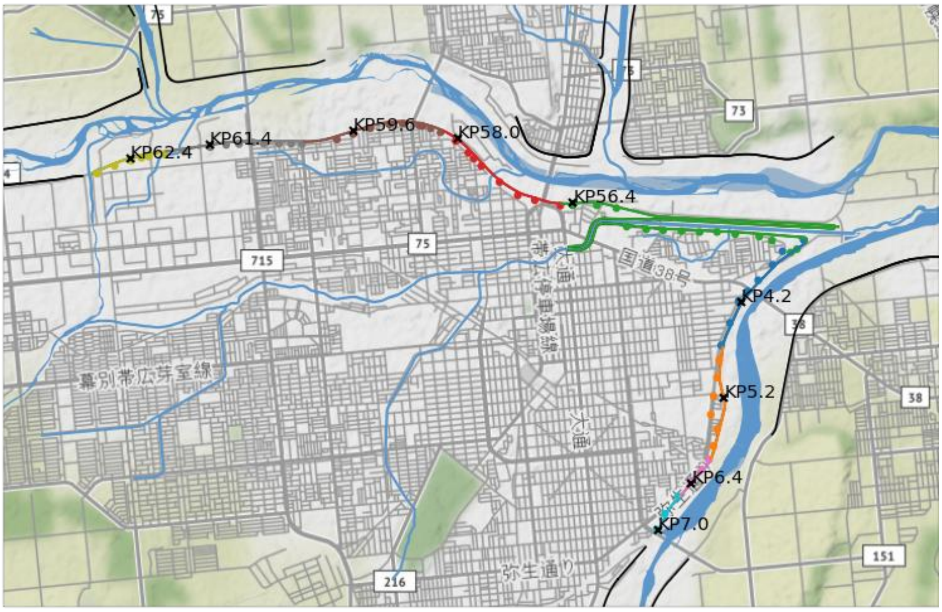

Figure 3
Overview of the KP-locations for which Qh, bank height and uncertainty data are available.

For clarity: Transects are drawn with an interval of 0.2 km along the river. These transects are denoted with KP X, with X being the longitudal distance. Data, such as rating curves and flood scenarios, are collected for each transect. The dikes are evaluated at each transect. The dike *segment* represents the part of dike related to the transect. As the consequences of a breach are likely similar for nearby transects, dike *sections* are defined, mostly consisting of 5 to 10 dike segments. The dike sections are denoted with the location of the segment that is used to calculate the flood consequences. For example, the brown section in the figure is denoted with KP59.6, which is the segment representative for the consequences of a breach at any point along the brown line.

4 Inner slope failure mechanism

In this study, we focused on the mechanism of levee failure caused by overflowing water, and adopted a method to determine the occurrence of levee failure based on the damage caused by erosion of the levee slope by overflowing floodwaters.

4.1 Dutch methods for grass revetment failure

In the Netherlands a cumulative damage approach is used to calculate revetment failure on the outer slope of the dike. On the inner slope a critical overtopping volume (without a duration aspect) is used. However, the critical values are derived from a cumulative damage approach, similar to the outer slope. In this study, we apply the cumulative overtopping approach to the inner slope as well. This means that during a storm event each overtopping wave adds a bit of damage to the total. When a certain threshold value is exceeded, the dike fails. We can write this in a formula as follows:

$$D = \sum_{i=1}^{N} \max[(\alpha_M(\alpha_a U_i)^2 - \alpha_S U_c^2); 0] \cdots 1$$

In which D is the cumulative damage, N is the number of waves. α_M and α_S are the model factor to take objects on the inner revetment into account (M for load, S for strength), for example trees that locally lead to more erosion. α_A is the factor for speeding up acceleration of the flow on the downward slope. U_i is the maximum depth average flow velocity for wave i. U_c is the critical flow velocity. Flow velocities larger than this critical level will cause damage to the revetment.

A problem with the approach from Equation 1, is that it is aimed at waves and not a continuous flow. There is no time component in the equation, just the number of waves and the maximum flow velocity in each of the waves. The number of waves can be translated to a time period, but a continuous flow cannot.

4.2 Cumulative overtopping damage for the inner slope

Another cumulative damage approach is described in [7]. They make a translation is between the overtopping/discharge towards flow velocities and duration. The general steps are as follows:

Based on the water level above the crest of the levee, the overtopping discharge can be calculated from the flow velocity on the crest of the levee:

$$u_0 = \sqrt{g h_0} \cdots 2$$
$$q = u_0 h_0 \cdots 3$$

This can be refined by using overflow formulas for (broad crested) weirs, but for simplicity we will stick with these formulas for now.

As the water flows over the dike, it will accelerate on the downward slope. Based on the shallow water equation simplified to steady flow, the terminal flow velocity can be calculated based on the slope and friction coefficient of the levee slope, as presented by Dean et al. (2010):

$$u_\infty = \left(\frac{8gq\sin\alpha}{f}\right)^{\frac{1}{3}} \cdots 4$$

This flow velocity can be compared to a critical flow velocity:

$$E_W = K_W(W_i - W_c)t_i = K_W\beta_W\left(u_{m,i}^3 - u_{c,W}^3\right)t_i \cdots 5$$

The W represents the physical quantity 'work', hence the power 3 for which the velocities above the critical flow velocities contribute to the damage. $E_W/K_W\beta_W$ is calculated to be $0.492 \cdot 10^6$ for a good quality grass cover. If the flow velocities are of such a magnitude that $\left(u_{m,i}^3 - u_{c,W}^3\right)t_i$ exceeds this value, the revetment fails. The critical flow velocity is calibrated on 1.80 m/s, which is low compared to the wave-oriented approach mentioned before.

With this approach, we can calculate the damage for all time steps. All different hydrograph shapes can be used in this way. The disadvantage of this method is that it does not take into account the more recent acquired knowledge on revetment strength. The method does however differentiate between grass cover qualities and provides standard deviations for the critical flow velocities.

An example for a hypothetical hydrograph shape and a good grass cover is shown in the figure below. The left figure shows the evolution of the water level. As soon as the water level is larger than the crest level, water will flow over the dike (middle figure). As the water level will accelerate on the inner slope, the flow velocity at the bottom is higher than on the crest. As soon as a critical flow velocity is exceeded, damage will start to accumulate (right figure). Failure occurs when the total damage exceeds a certain threshold.

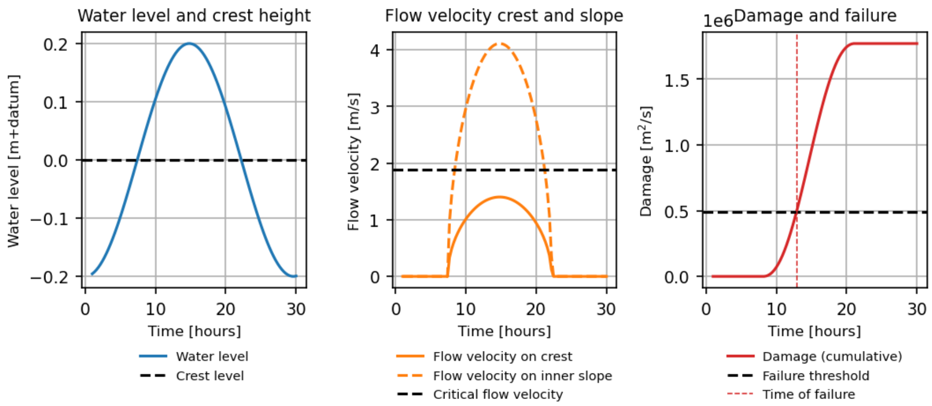

Figure 4
Example of calculating damage due to overflow with a cumulative overtopping approach.

4.3 Fragility curves: failure probability given water level

Following these steps for different water levels (and with a schematised hydrograph shape), gives the failure probability for each of the water levels. Without further uncertainty, this is 0.0 when the water level causes a total damage lower than the critical amount, or 1.0 when higher. In reality, a lot of the model parameters are uncertain, resulting in a more gradual fragility curve from 0.0 to 1.0 [10]. These uncertainties are explained in the next chapter.

5 Sources of uncertainty

Last chapter described the method for determining a relation between water level and dike failure (i.e., the fragility curve). In a fully deterministic setting, there is a specific water level at which the failure probability jumps from "no failure" (0.0) to "failure" (1.0). In reality, several uncertainties cause this relation to be more diffuse. This chapter described the quantification of these uncertainties.

The following image shows the different uncertainties we consider for the failure mechanism overflow: the damage (or critical overtopping velocity, as described in the last section), the water level and the crest height.

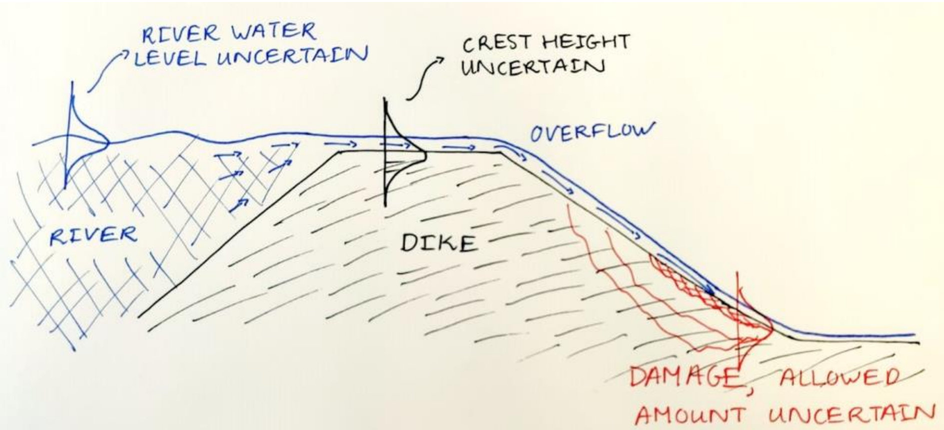

Figure 5
Sketch of overflow with the uncertain variables indicated.

5.1 Water levels

For each KP-location (shown in Chapter 3), a relation between discharge Q (or flow rate) and water level h is available. This formula was provided by the Hokkaido Development Bureau. It was developed based on the results of runoff calculations and the water level and flow rate at the observation stations. We call these rating curves or HQ-relations. The figure below shows the water levels from these relations, for different discharges, as well as the design bank height.

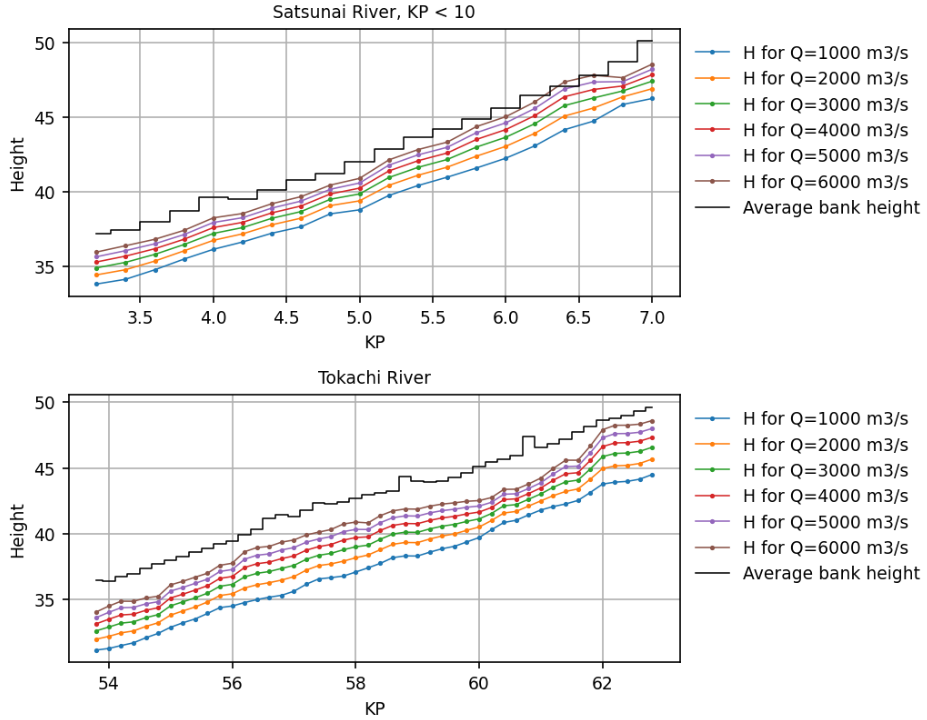

Figure 6
Design bank height and water level for a number of discharges

Uncertainty in river levels was evaluated based on the relationship between water levels calculated from the rating curves and water levels observed in the field in the target river. Observations were collected at Obihiro, Tokachi River (KP56.73) and Nantaibashi, Satsunai River (KP15.00). The data are available for five years from 2014 to 2018. Observations were carried out once a week or during high runoff. The difference between the observed water level and the water level calculated from H-Q-relation to the observed flow were gathered. The mean and variance of these differences were then used to quantify the uncertainty. This is illustrated for both locations in the figures below.

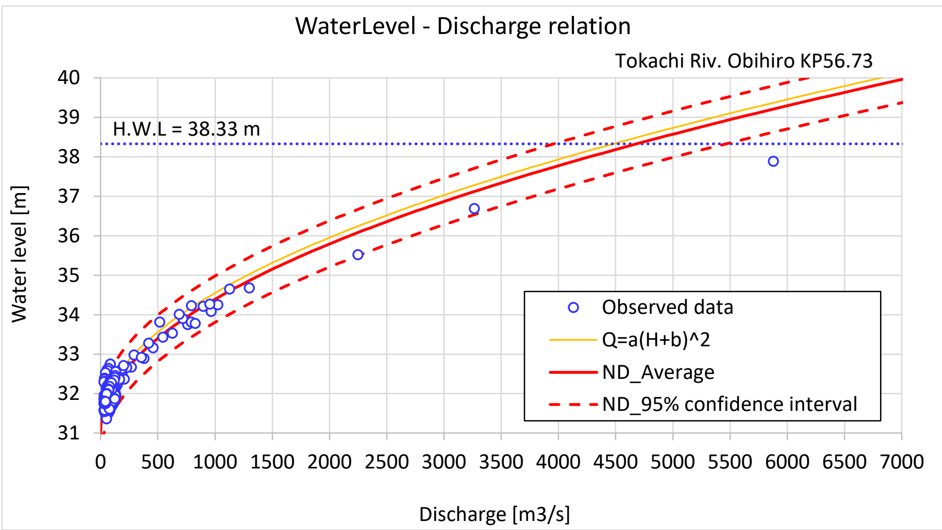

Figure 7
Calculation of water level dispersion at Obihiro point (KP56.73)

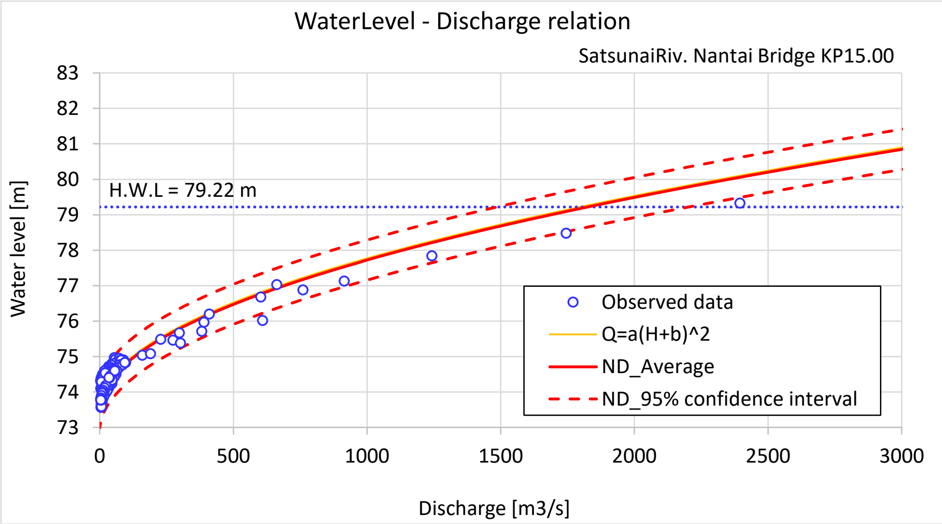

Figure 8 Calculation of water level dispersion at Satsunai point (KP15.00)

Table 1 Average and variance of the difference between observed water levels, and water levels from the rating curves.

Location	Average [m]	Variance [m]
Tokachi KP56.73	-0.1601	0.2937
Satsunai KP15.00	-0.0511	0.2831

When evaluating the uncertainty, the results from Obihiro site were applied to the Tokachi River and the results from Minami Obi Bridge site were applied to all sections of the Satsunai River.

5.2 Bank Height

The high water level set in the river plans for the Tokachi River and the Satsunai River is defined as the "design bank height. The height of the top of the embankment is organized longitudinally based on the ground level data (LP data) obtained from aerial laser surveying, and the mean value and standard deviation are calculated every 0.2 km in the longitudinal direction of the embankment to be used as the uncertainty of the embankment height. The levee height and LP data in the plan were provided by the Hokkaido Development Bureau.

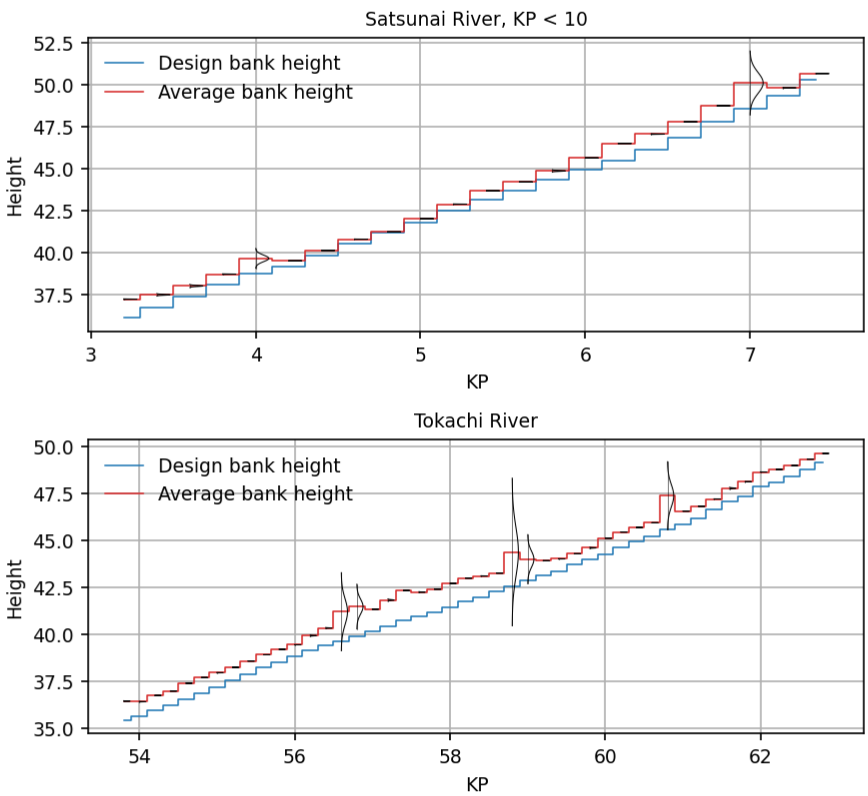

Figure 9
Design bank height and average bank height with uncertainty

For most locations the uncertainty in the bank height is very small. However, for some locations the bank height is higher than the average bank height, which also gives a large deviation. In reality, this deviation is skewed towards positive values (the actual height being larger than the design height), but in our approach a normal distribution is used. This leads to large probabilities of a relatively low bank height, resulting in too high failure probabilities. We advise to fit a different probability distribution to the differences in future research.

5.2.1 Water level and crest level uncertainties

The relation between water level and discharge (i.e., the rating curve) can change from event to event. This can be due to bed erosion or sedimentation, or hydrodynamic effects like hysteresis. Additionally, the crest level, with a similar effect as water level uncertainty, is not exactly known. Both uncertainties can combined into a single variable; the uncertainty in "the difference between water level and crest level".

5.3 Critical flow velocities

In the cumulative overtopping approach described in Chapter 4, the standard deviations of the critical flow velocities are given. These can be used to quantify uncertainty on the strength side:

- For "plain grass - good cover": μ_{u_c} = 1.80 m/s, σ_{u_c} = 0.38 m/s
- For "plain grass - average cover": μ_{u_c} = 1.30 m/s, σ_{u_c} = 0.12 m/s

- For “plain grass - poor cover”: μ_{u_c} = 0.76 m/s, σ_{u_c} = 0.04 m/s

In our approach, the condition of plain grass is "good cover" because the dikes in the Tokachi River are properly managed.

5.4 Combining the uncertainties

The different uncertainties (random variables) can be combined into a single fragility curve. We used Monte Carlo simulations to calculate a fragility curve that takes into account uncertainty.

Integration into the fragility curve was done by Monte Carlo simulation. The evaluated uncertainties, water level, levee height, and levee slope conditions, were given as random numbers following a normal distribution with their respective means and standard deviations. Equation 6 represents the probability density function of the normal distribution. For the peak water level, the peak flow rate of the target hydrograph was converted to water level using the HQ-relation (Equation 7), and the standard deviation of the HQ-relations organized in the previous section was used for the water level to derive a random number following a normal distribution (Equation 8). Similarly, for the embankment height, the standard deviation of the difference between the planned and actual embankment height was used to derive a random number according to the normal distribution (Equation 9).

$$f(x) = (2\pi\sigma^2)^{-1/2} exp\left(-\frac{1}{2\sigma^2}(x-\mu)^2\right) \cdots 6$$

$$H_{peak} = \sqrt{\frac{Q_{peak}}{a}} - b \cdots 7$$

$$h_{peak} \sim N(H_{peak}, \sigma_{H-Q}) \cdots 8$$

$$h_{bank} \sim N(H_{bank}, \sigma_{bank}) \cdots 9$$

If $h_{peak} > h_{bank}$,. the overflow flow rate is calculated from Equations 2 and 3. After this, the flow velocity at the embankment slope is calculated with Equation 4. Finally, Equation 5 is used to determine if the damage exceeds the threshold for levee failure. The state of the slope in Equation 5 also uses a random number following a normal distribution.

The above operation was repeated 5,000 times for each dike segment and water level, and the probability of breaching was calculated from the frequency of the number of times that the embankment was expected to be breached (i.e., total damage exceeding the critical damage). For illustration, two of these iterations are shown in the figure below.

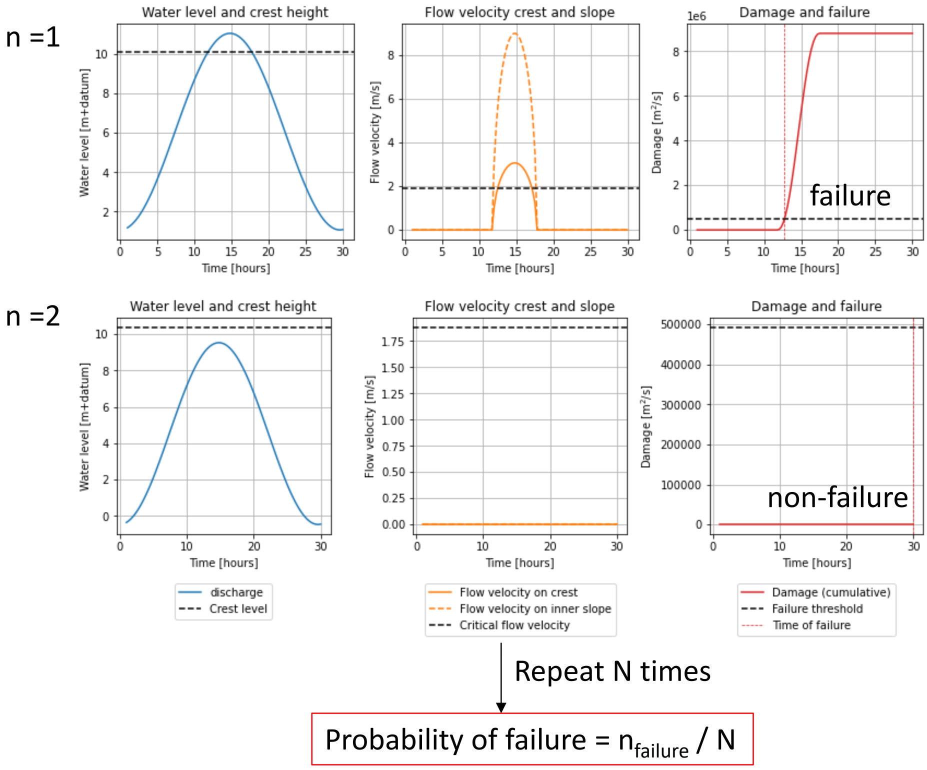

Figure 10
Flow of calculating dike failure probability using Monte Carlo simulation.

6 Bank failure probability

In this chapter, we calculate the probability of levee failure using the method of creating fragility curves from Chapter 4, and the described uncertainties in Chapter 5. First, the levee failure probabilities are calculated at intervals of about 0.2 km. Next, the breach probabilities for each predefined section are organized to provide data for the risk assessment of WP3. Finally, the failure probability of the levee is also calculated for the situation in which failure of upstream sections is taken into account.

6.1 Calculate failure probabilities

The failure probabilities of levees in the Tokachi River and the Satsunai River were calculated. The failure probabilities were calculated at intervals of about 0.2 km. As a result, the failure probability of the levees of the Satsunai River ranges from about 10^{-5} to 10^{-3}. The failure probabilities of the levees of the Tokachi River are in the range of 10^{-5} to 10^{-3}, similarly to Satsunai River, although they varied greatly by location.

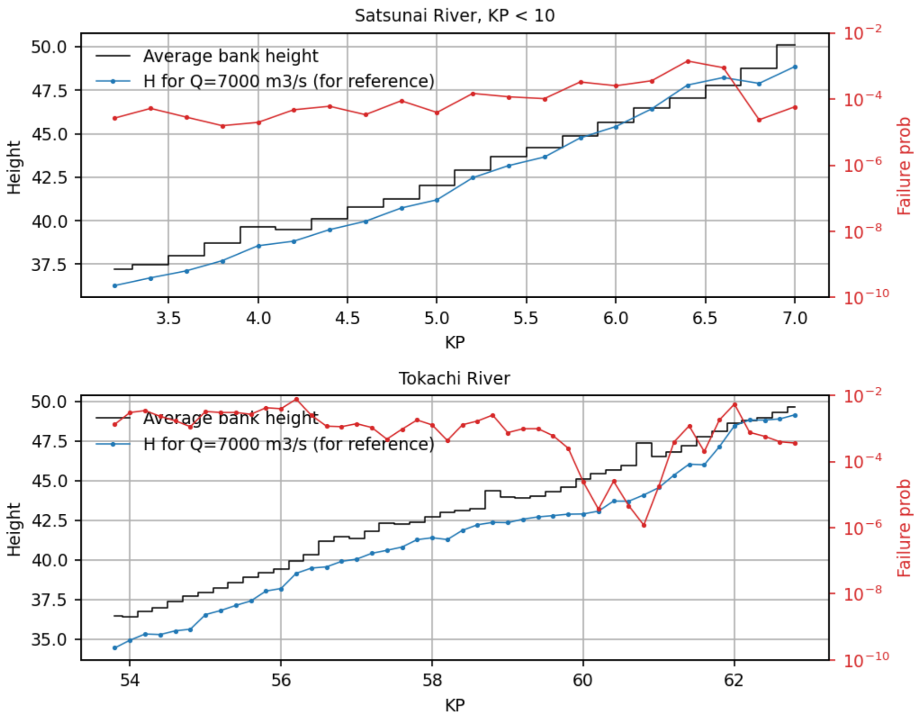

Figure 11 Failure probability per location (KP). The design bank height and a high water level are shown for reference

6.2 Combine segments to sections

Until now, the failure probabilities where calculated for a levee segment. In this section we combine the failure probabilities from segments, to sections, to the whole of Obihiro (recall that the definition of segments and sections is explained in Chapter 3). When doing so, we want to avoid counting the consequences of the same flood scenario multiple times. This means that a failure of one segment, reduces the failure probability of a next section, unless the conditions for which they fail are independent. Combining the failure probabilities means that we make a realistic choice between combining probabilities dependent and independent.

- First of all, we combine the probabilities conditional to the discharge. This means we assume that a single high discharge causes a high water level along all flood defenses. This might be a little simplified for the two rivers (Satsunai and Tokachi), but is probably a very realistic simplification, as the high water levels are caused by the same rain event..
- Secondly, segments are grouped into sections based on similar consequences. Because these sections are close to each other, we assume the strength to be dependent. This means that the dike will always fail at the segment with the highest failure probability (for that discharge).
- Thirdly, sections are combined per river branch independently (still conditional to discharge), but we take the order of the sections into account. Sections are far enough apart for the strength of the dike to be considered independent. However, when an upstream sections has failed, we assume the water level to be reduced such that the downstream dikes cannot fail anymore during this event.

To make this as specific as possible, we express it with a mathematical notation. Combining failure probability per section:

$$P_{f,section}|q = \max_{i=1}^{n}(P_{f,segment,i}|q)$$

In which $P_{f,section}$ is the section failure probability, and $|q$ means conditional to discharge q. $P_{f,segment,i}$ is the failure probability of segment i. There are n segments in the section.
Combine sections into a total failure probability is done in upstream to downstream order (1, 2, 3, …, n):

$$\begin{aligned}
&P_{f,scenario,1}|q = P_{f,indep,1}|q \\
&P_{f,scenario,2}|q = P_{f,indep,2}|q \cdot [1-(P_{f,scenario,1}|q)] \\
&P_{f,scenario,3}|q = P_{f,indep,3}|q \cdot [1-(P_{f,scenario,1}|q + P_{f,scenario,2}|q)] \\
&P_{f,scenario,n}|q = P_{f,indep,n}|q \cdot [1-sum_i^{n-1}(P_{f,scenario,n}|q)]
\end{aligned}$$

With $P_{f,scenario,1}|q$ we express the *scenario* failure probability, which is corrected for potential upstream failures. It is called the scenario probability, because it can be assigned to the consequences of a flood scenario. $P_{f,indep,1}|q$ is the independent section failure probability, so without taking upstream flooding into account.
For the most upstream section, the scenario and independent failure probability are the same, as no flooding further upstream is considered. For the second section, the failure probability is reduced, since failure can only

take place when the upstream section has not failed. For the third section, both upstream sections reduce the flood risk, etcetera.

6.3 Segment probabilities

The result of combining segment probabilities to sections is shown in the figure below. Per discharge the maximum failure probability is selected, resulting in the black curve. For most sections a single segment is dominant, only for section KP59.6 (lower centre in Figure 12) two sections result in a combined fragility curve.

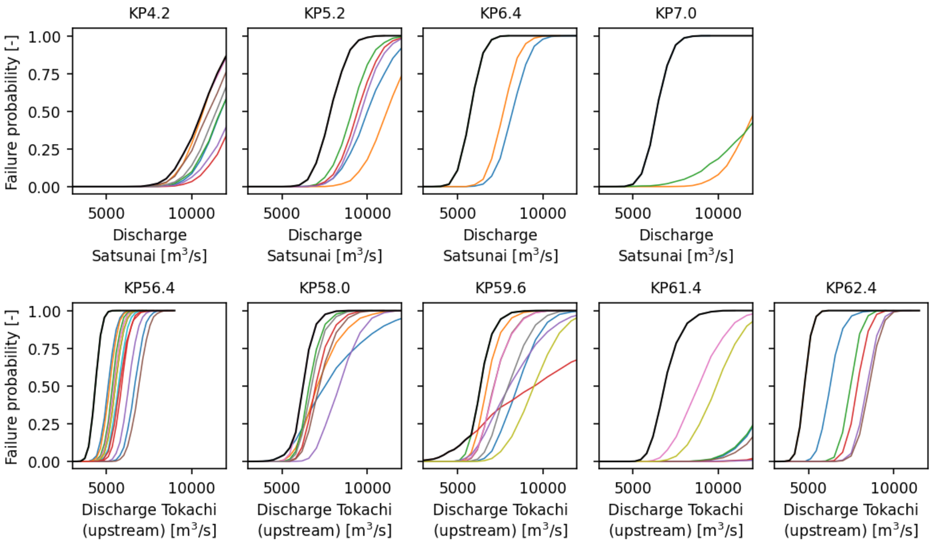

Figure 12 Fragility curves for all segments (colored), and the combined section curve (black).

6.4 Combining section probabilities per river branch

The result of combining section probabilities per river branch, is shown in the two figures below. The black curves are the original section curves, independent of upstream sections. The red dashed curves are after taking potential failure of upstream sections into account. The highest discharges will certainly lead to upstream failure, reducing the conditional failure probabilities downstream for these discharges. Therefore, downstream sections will only fail at relatively low discharges, especially if the section has a higher failure probability.

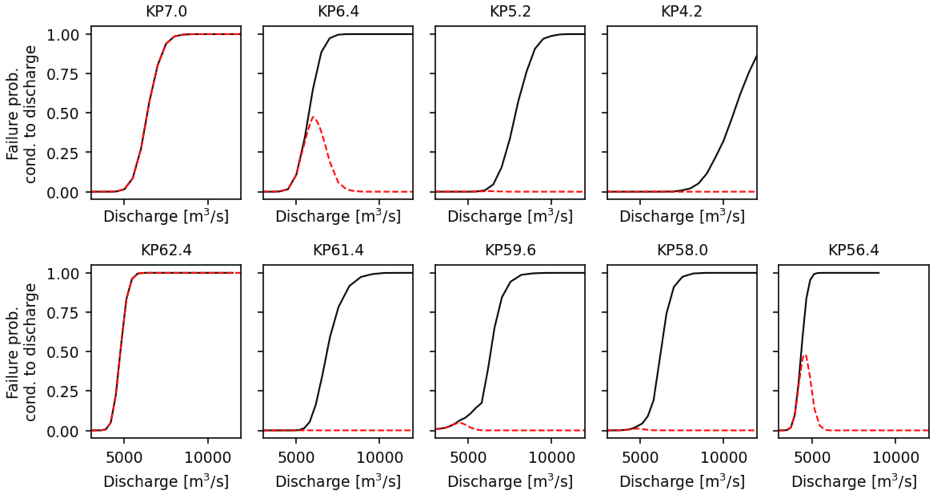

Figure 13 Fragility curves for all sections of Tokachi river, before and after taking the effect of upstream sections into account.

6.5 Comparing the calculated failure probabilities

To show the sensitivity of the total failure probability to the method with which we calculated it, we calculate the total failure probability with full dependence, full independence and the applied method (mix of dependence and independence).

Table 2 Total failure probability for the applied method, compared to the fully dependent and independent situation.

Approach	Failure probability
Full dependence	0.00883
Applied method (partial dependence)	0.02564
Full independence	0.07476

The applied method is more or less in between the independent and dependent situation. Note that these probabilities are calculated for the "Future" scenario and the "average" discharge statistics. For a different combination

7 Flood probabilities

The method for calculating the flood probability is extensively described in chapter 2. Here, a short overview of the steps leading from discharge statistics (WP1) to consequences (WP3) is given.

- WP1 calculates the exceedance probabilities of the discharges for Satsunai and Tokachi river. Additionally, information on the hydrograph shapes is provided. This is used to define a number of hydrograph classes, with different flood durations.
- Fragility curves give a relation between a water level and a failure probability conditional to that water level. It is therefore a measure of the strength of the dike. In WP2 we calculate these curves for the failure mechanism overtopping. We take into account:
  - that the duration of overtopping affects the failure probability. Different hydrograph classes give different fragility curves.
  - The uncertainty in the revetment quality, revetment height, and the water levels. With a Monte Carlo simulation these uncertainties are incorporated in the fragility curve.

  This gives a failure probability per dike segment, dependent on the hydrograph class. Calculating these is the main goal of WP2.
- WP3 focusses on calculating the flood risk, by combining the flood probabilities with the damage and loss of life it causes. Many of the sections will fail under the same conditions. However, if one segment fails, it is less likely that the others will still fail. We need to consider this, to avoid overestimating the calculated flood risk. We do this by correcting the fragility curves of downstream sections for potential upstream flooding.

7.1 Discharge statistics

The discharge statistics are determined within work package 1 (WP1). The results from that work package are used in this work package to determine the flood risk in WP3. In this chapter a short summary is given on the flood probability. More details on determining flood probabilities can be found in the report on WP1.

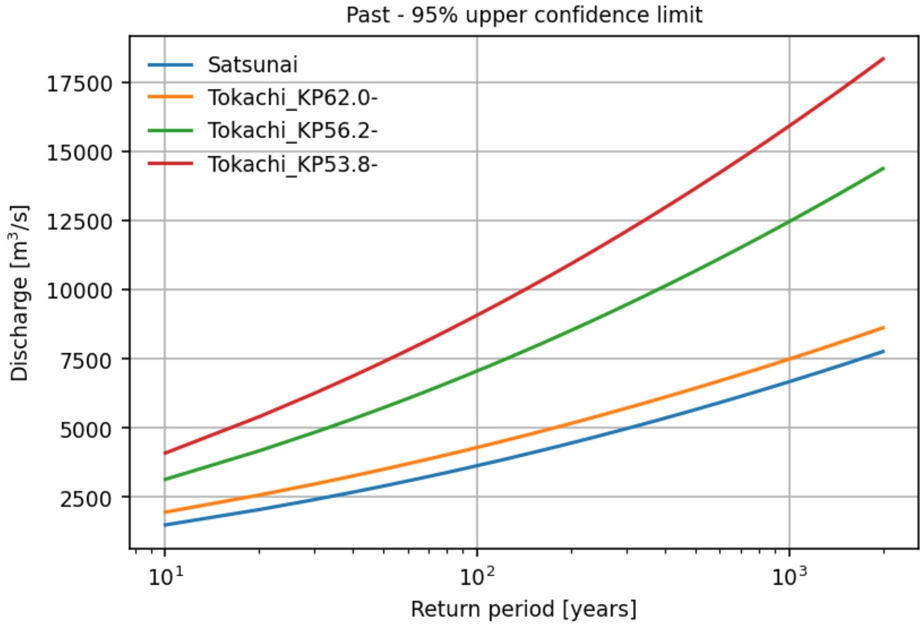

Figure 14
Discharge statistics of Past simulation

7.2 Flood probability

The flood probability was calculated using the method explained in Chapter 6, using the exceedance probabilities of the discharge calculated in WP1. The flood probability was calculated for each section that is used WP3. It is a measure of the safety of the dike section, and is shown in the middle column of the table below. Because upstream failure reduces the probability of failure for downstream sections, also the *scenario* probabilities are calculated in which this is taken into account. These are the probabilities that are used in WP3. The probabilities in the four tables below are for the average discharge statistics and upper limit, as well as for the past scenario without climate change and the future scenario.

Table 3
Past, average
Failure probabilities for the sections used in WP3. The scenario probabilities are the failure probabilities after correcting for upstream failure.

Location	Section failure probability	Scenario probability
Satsunai KP7.0	2.53e-05	2.53e-05
Satsunai KP6.4	5.67e-05	3.79e-05
Satsunai KP5.2	4.62e-06	1.45e-07
Satsunai KP4.2	3.00e-07	6.52e-10
Tokachi KP62.4	1.41e-04	1.41e-04
Tokachi KP61.4	3.36e-04	9.93e-07
Tokachi KP59.6	1.21e-03	5.36e-04
Tokachi KP58.0	6.62e-04	4.49e-05
Tokachi KP56.4	2.04e-02	1.06e-02

Table 4
Past – upper bound
Failure probabilities for the sections used in WP3.

Location	Section failure probability	Scenario probability
Satsunai KP7.0	1.36e-03	1.36e-03
Satsunai KP6.4	2.11e-03	9.30e-04
Satsunai KP5.2	5.42e-04	3.75e-06
Satsunai KP4.2	1.22e-04	1.07e-08
Tokachi KP62.4	6.85e-03	6.85e-03
Tokachi KP61.4	1.36e-02	7.25e-06
Tokachi KP59.6	1.98e-02	2.31e-03
Tokachi KP58.0	1.76e-02	2.64e-04
Tokachi KP56.4	8.52e-02	1.66e-02

Table 5
Future – average
Failure probabilities for the sections used in WP3.

Location	Section failure probability	Scenario probability
Satsunai KP7.0	8.87e-04	8.87e-04
Satsunai KP6.4	1.42e-03	6.52e-04
Satsunai KP5.2	3.26e-04	2.75e-06
Satsunai KP4.2	6.11e-05	3.37e-08
Tokachi KP62.4	5.46e-03	5.46e-03
Tokachi KP61.4	9.52e-03	5.72e-06
Tokachi KP59.6	1.55e-02	2.07e-03
Tokachi KP58.0	1.37e-02	2.56e-04
Tokachi KP56.4	7.53e-02	1.60e-02

Table 6
Future – upper bound
Failure probabilities for the sections used in WP3.

Location	Section failure probability	Scenario probability
Satsunai KP7.0	1.47e-02	1.47e-02
Satsunai KP6.4	1.99e-02	6.27e-03
Satsunai KP5.2	7.99e-03	2.86e-05
Satsunai KP4.2	3.05e-03	3.49e-07
Tokachi KP62.4	5.30e-02	5.30e-02
Tokachi KP61.4	7.86e-02	1.57e-05
Tokachi KP59.6	9.38e-02	3.46e-03
Tokachi KP58.0	9.16e-02	5.66e-04
Tokachi KP56.4	2.09e-01	1.88e-02

8 Sensitivity analysis

The failure probabilities calculated in this study are subject to the quantification of the uncertainties. In this chapter, we first compare the sensitivity of the parameters discussed in Chapter 5. Additionally, the assumed hydrograph shape is compared to simulated shapes.

8.1 Uncertainty in bank height, crest level and rating curve

In this study, three factors are considered as random variables. The first is the relationship between water level and river discharge, the second is the height of the embankment, and the third is the condition of the embankment slope. Here, we conducted a sensitivity analysis to see how much the three uncertainties affect the probability of levee failure.
The method of sensitivity analysis is based on the following conditions:

1. When all three uncertainties are taken into account
2. when only one item of each is considered (three cases)
3. When no uncertainty is taken into account

The analysis was conducted for the Tokachi River Obihiro site (KP56.7) as a representative.
In the case of including the three uncertainties, the failure probability is distributed between 10,500 m^3/s and 12,000 m^3/s. In the case of including only H-Q uncertainty, the distribution is almost the same range. On the other hand, in the case of including only Grass Condition and the case of including only Bank Height, the distribution is in the range of 11150m^3/s to 11300m^3/s. This range is narrow and close to the range of cases where uncertainty is not taken into account. These results indicate that the uncertainty of water level and discharge had a significant effect on the probability of levee failure at this point.
From the sensitivity analysis, it is possible to analyze the uncertainties that affect the failure probability. It is also possible that uncertainties with small impact may not need to be considered.

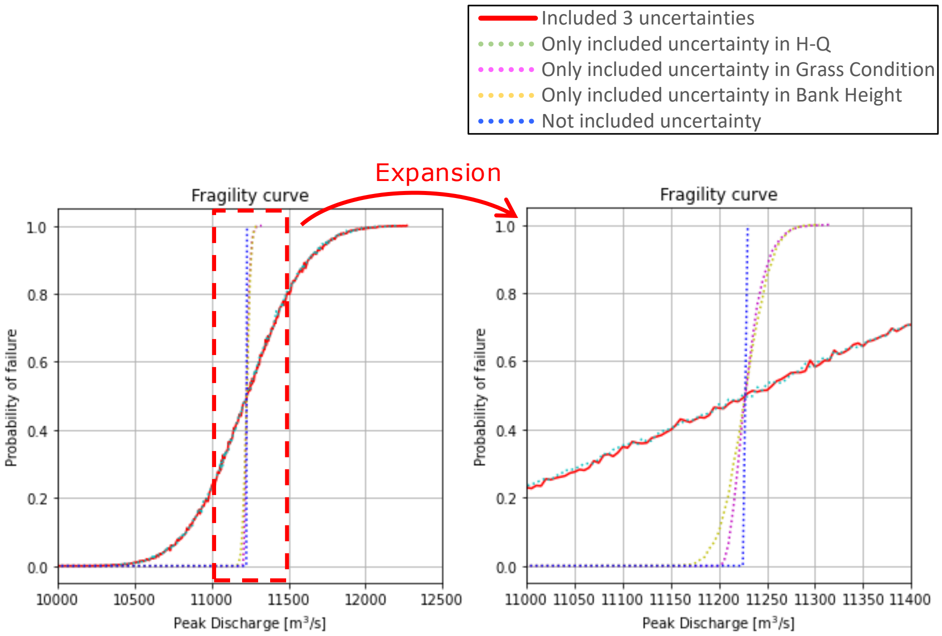

Figure 15
Comparison of Fragility Curves by Included Uncertainties

8.2 Hydrograph shape

In this pilot project we assumed a cosine-shaped water level time evolution to calculate the overflow over the dike and resulting revetment damage. In this section we discuss the implications of the assumed shape, by comparing the cosine shape to a set of hydrographs along Satsunai river. To be specific, the hydrographs before flooding, in between KP002.80 and KP024.60. In the analysis, we consider a peak discharge of 4000 m^3/s, and overflow for discharges higher than 2000 m^3/s. In reality, overflow happens at a certain water level, but for simplicity we consider only the discharges, without converting them to water levels.

The first step is to collect all hydrographs with a peak discharge in between 3500 and 4500 m^3/s, as is shown in the figure below on the left. The range is a trade-off between number of hydrographs and consistency (similar peak discharge). In the second step, we shift the hydrographs to the same peak moment, as is shown on the right in the figure below.

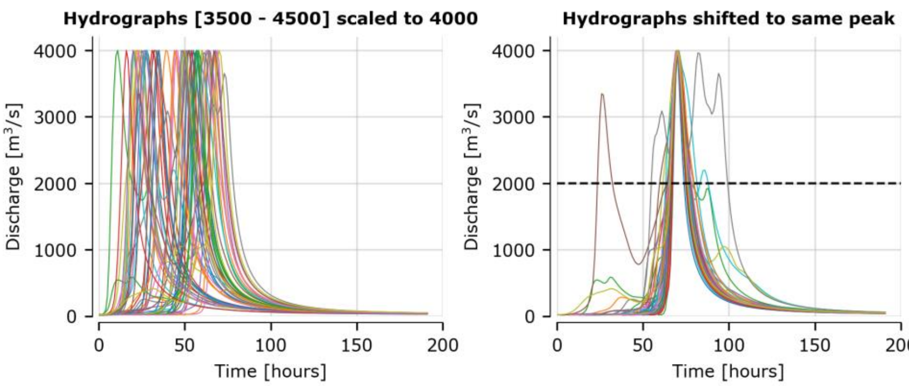

Figure 16
Left: hydrographs between 3500 and 4500 m^3/s, scaled to 4000 m^3/s. Right: the same hydrographs, now also shifted to the same peak moment.

We classify the duration of each hydrograph, by considering the duration that the discharge is higher than the overflow discharge of 2000 m^3/s. The histogram of these durations is shown below:

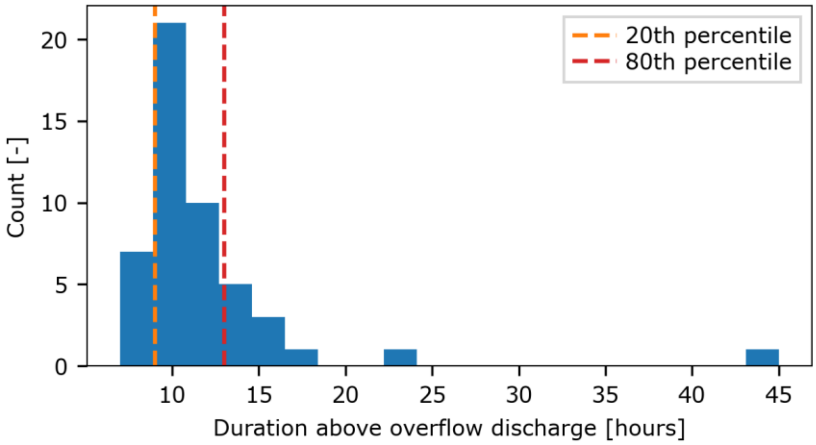

Figure 17
Histogram of duration above the overflow discharge level, for all selected hydrograph.

Based on these durations, the hydrographs are divided into three bins: the lowest 20% of the overflow durations, the middle 60% and the highest 20%. For each of these classes, we calculate an average hydrograph shape, by calculating the average discharge at each time step within the class. The result for this is shown in the figure below. In this figure also the used schematized cosine shape is shown.

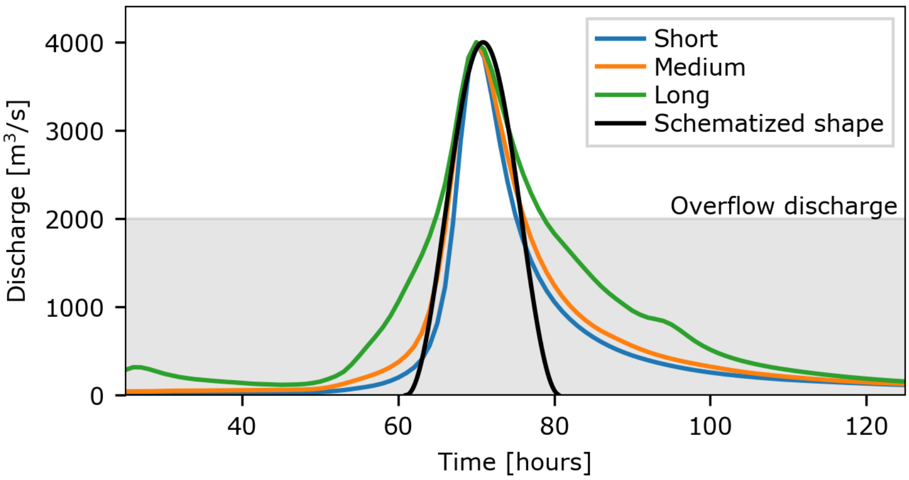

Figure 18
Left: hydrographs between 3500 and 4500 m^3/s, scaled to 4000 m^3/s. Right: the same hydrographs, now also shifted to the same peak moment.

The variation in hydrograph shapes between the three classes is not too big, as we already saw in the histogram. The schematized shape is a good model for the peak of the hydrograph shape, which is the part that matters most for the dike safety.

Although we did not explicitly calculate the effect of the uncertainty in overflow duration, we can assume, based on this quick analysis, that the hydrograph shape has a relatively small effect on the failure probability. For different locations or river branches, these result might differ. Another point of attention is that the average per time step we used, averages out secondary peaks, as the one shown on the right in Figure 16. In a next project the sensitivity of the hydrograph shape could be analysed further, and even be taken into as a random variable.

8.3 Concluding

Of the sources of uncertainty that were discussed in Chapter 5, the uncertainty in the rating curve has the largest effect on the failure probability.

9 Discussion

In this section, the probability of levee failure and flood occurrence is discussed in terms of the results of the calculation method approach.

9.1 Failure Probability

According to the calculation results of the probability of levee failure, the probability of levee failure near KP60.8 of the Tokachi River is small, about 10^{-6}. This may be due to the fact that this section includes a bridge and is relatively high compared to the sections before and after it. On the other hand, the probability of levee failure near KP58.8 of the Tokachi River is relatively higher than that of the sections before and after it. Although the average height of the embankment is high due to the inclusion of the bridge, the difference in the height of the embankment between the bridge and the section before and after the bridge is large, and the uncertainty of the height of the embankment within the section is thought to have influenced the increase in the probability of embankment failure. This point needs to be accurately evaluated in the future by assessing the uncertainty as only positive variability.
The results of the uncertainty sensitivity analysis indicate that the water level-flow relationship has a significant effect on the probability of levee failure at the target locations. The relationship between water level and flow is due to the temporal changes in the riverbed topography. It changes with each outflow as well as with time during the outflow. This result is considered to represent the flood characteristics of the target watershed, which is characterized by high flow velocity and large water level changes.
Three uncertainties are taken into account in the probability of levee failure. It is unclear how much influence this uncertainty has on the risk assessment in WP3. If the impact on the outcome of the risk assessment is small, the uncertainty here may be negligible. On the other hand, if the impact is large, it may be necessary to reconfirm the factors that cause uncertainty and conduct sensitivity analysis of the data. In the future, we believe that a sensitivity analysis of the uncertainty of the calculation results of each WP to the risk assessment results should be conducted.

9.2 Flood probability

As for the flood probability, within a section of the same river with the same planned size (discharge), the results showed that the levee failure probability was larger upstream and smaller downstream. For example, in the section of the Tokachi River after the confluence of the Shikaribetsu River (from KP59.6 to KP56.4), the return period was about 1.5×10^{3} years upstream and about 4.5×10^{6} years downstream. In the Satsunai River, the return period is about

3.0 x 10^3 years in the upstream side and about 4.9 x 10^6 years in the downstream side. This result is due to the fact that the failure probability of the upstream bank is deducted when calculating the failure probability of the downstream bank.
The hazard maps published in Japan show inundation damage based on the planned size of the river and the assumed maximum external force. The condition for a levee failure is an exceedance of the planned elevation. The results of the inundation analysis are superimposed on the results of the inundation analysis for all the assumed breach points. In other words, the level of safety of levees is uniform, and levee breaches are considered as independent phenomena. This method can provide residents with a safer assessment of the hazard. On the other hand, when quantifying damage for the purpose of flood risk assessment, there is a possibility of overestimation. The approach in this study adopts a non-independent approach that expresses the probability of levee breaches at each location in a probabilistic approach and takes into account the occurrence of levee failures upstream. As a result, this method expresses the probability of flood occurrence in a more realistic way. In the future, quantitative flood risk assessment will be required to promote flood control measures in flood plains. By adopting the method proposed in this study, more accurate flood risk assessment will be possible.

10 Conclusions and Recommendations

The results of this study are described below.

- A probabilistic assessment of levee failure was conducted for levees in the Tokachi River basin, targeting the phenomenon of levee failure due to overtopping. We proposed to incorporate three uncertainties related to the process of levee failure in the probabilistic assessment. The first is the relationship between water level and flow rate, the second is the relationship between the planned high water level and the actual levee height, and the third is the condition of the levee slope.
- The probability of levee failure at each evaluation point was calculated and the results were integrated in several sections. We proposed an approach to calculate the downstream levee breach probability by considering the upstream levee failure probability in the integration.
- Combined with the exceedance probability of flow provided by WP1, the flood probability was calculated. As a result, the maximum and minimum flood probabilities were found to be about 1.6×10^{3} and 2.4×10^{8}, respectively, in the vicinity of the targeted Obihiro urban area.

The approach proposed in this study is expected to contribute to the study of flood control measures based on quantitative inundation risk assessment in the target watershed. The future research items proposed in the study are as follows.

- In this study, levee failure due to overtopping is the subject of evaluation. In this study, we focused on levee failure due to water overtopping, but there are some reports of levee failure due to erosion and piping in Japan. Therefore, the probability of levee failure due to other levee failure mechanisms should be evaluated in the future.
- In this study, flood hydraulics are calculated assuming a model waveform. Flood runoff in Japan is characterized by various shapes of hydrographs, which are expected to affect the probability of levee failure and damage during inundation. Therefore, the flood probability should be evaluated taking into account the shape of the hydrograph.

11 References

[1] Obihiro Development and Construction Department, Hokkaido Regional Development Bureau, Report of flood in August, 2016. (Japanese Only)

[2] Interagency Performance Evaluation Task Force: Performance Evaluation of the New Orleans and Southeast Louisiana Hurricane Protection System - Final Report, Volume VII, pp.108-109, US Army Corps of Engineers, 2007.

[3] Water and Disaster Management Bureau, Ministry of Land, Infrastructure and Transport, The Guide for Analysis of Flood Damage Indicators (2013 trial version), 2013, https://www.mlit.go.jp/river/basic_info/seisaku_hyouka/gaiyou/hyouka/pdf/higaisihyou_h25.pdf . (Japanese only)

[4] Ikeushi, K. et al., Inundation Patterns and Fatality Analysis on Large-scale Flood, Journal of Japan Society of Civil Engineers. Ser. B1, Hydraulic engineering, Vol.67, No.3, pp133-144, 2011. https://www.jstage.jst.go.jp/article/jscejhe/67/3/67_3_133/_article/-char/ja/ (Japanese Only)

[5] Jonkman, S.N., Loss of life estimation in flood risk assessment: Theory and applications, 2007, https://repository.tudelft.nl/islandora/object/uuid%3Abc4fb945-55ef-4079-a606-ac4fa8009426 .

[6] Water and Disaster Management Bureau, Ministry of Land, Infrastructure and Transport, Technical Review Board for River Embankments Based on the Damage Caused by Typhoon No. 19 in 2019, 3rd Meeting, Document 2, 2020, https://www.mlit.go.jp/river/shinngikai_blog/gijutsu_kentoukai/dai03kai/pdf/doc2.pdf. (Japanese only)

[7] Dean, R. G., Rosati, J. D., Walton, T. L., & Edge, B. L. (2010). Erosional equivalences of levees: Steady and intermittent wave overtopping. Ocean Engineering, 37(1), 104-113.

[8] Jongejan, R. B., & Maaskant, B. (2015). Quantifying flood risks in the Netherlands. Risk Analysis, 35(2), 252-264.

[9] Slomp, R., Knoeff, H., Bizzarri, A., Bottema, M., & de Vries, W. (2016). Probabilistic flood defence assessment tools. In E3S Web of Conferences (Vol. 7, p. 03015). EDP Sciences.

[10] Van der Meer, J. W., Ter Horst, W. L. A., & Van Velzen, E. H. (2009). Calculation of fragility curves for flood defence assets. Flood Risk Management: Research and Practice, 567-573.

Head office
HKV
Botter 11-29
8232 JN Lelystad
The Netherlands

Branch office
Informaticalaan 8
2628 ZD Delft
The Netherlands

0320 294242
info@hkv.nl
www.hkv.nl/en/